Refractive Index of Graphite and Graphene at Wavelengths Spanning the Carbon K-edge

H. Wahab[a], C. Jansing[b], H.-Ch. Mertins[b], S.-H. Choi[c] and H. Timmers[a]

[a] *School of Physical, Environmental and Mathematical Sciences, University of New South Wales in Canberra, PO Box 7916, Canberra BC 2610, Australia.*
[b] *Department of Engineering Physics, Münster University of Applied Science, Stegerwaldstraße 39, Steinfurt, Germany.*
[c] *Department of Applied Physics and Institute of Natural Sciences, Kyung Hee University, Yongin 446-701, Korea.*

Near edge x-ray absorption fine structure spectroscopy was performed to determine the imaginary part of the refractive index of graphite and graphene at wavelengths spanning the carbon K-edge. The real part of the refractive index has been derived from this measured imaginary part via piecewise polynomial Kramers-Kronig transformations. This paper presents the first comparison of simulated reflection spectra using these data with measured reflection spectra.

1. Introduction

The refractive index (RI) is an important parameter in photon-matter interactions and it is paramount when designing x-ray optics such as mirrors or waveplates. The soft x-ray RI of amorphous carbon, which is typically used as spacer material in x-ray mirrors, has been determined in the past using an interferometer [1] or with reflectivity measurements [2]. However, the high attenuation of soft x-rays at the K-edge makes such measurements difficult. Furthermore surface roughness and carbon contaminations in the light path need to be carefully considered for accurate results. No such measurements are available of the RI for highly oriented pyrolytic graphite (HOPG).

Recently, Yan *et al*. [3] have demonstrated the determination of the RI of polymer films across the carbon K-edge using doubly-subtracted Kramers-Kronig (KK) transformations and achieved considerable accuracy in deriving the density of the films with a least-squares fit. Motivated by this success, in this work, an algorithm by Watts [4] has been applied to attempt the determination of the RI of HOPG and that of graphene. This novel approach utilizes the fact that Near Edge X-ray Absorption Fine Structure Spectroscopy (NEXAFS) of both carbon materials can readily be performed. The validity of the extracted RI can then be verified by simulating reflection spectra and compare them with experimental reflectance data.

2. Set-up and Method

NEXAFS measurements were performed at the soft x-ray beam line of the Australian Synchrotron, Melbourne [5]. Linearly polarised photons with a high spectral resolution of $E/\Delta E$ = 6000 at 300 eV were focused to a 100 μm x 40 μm spot on the sample. The measurements spanned the energy range of 280 – 320 eV.

Reflection spectroscopy was performed with the polarimeter [6] at the PGM-2 beamline of BESSY II, Berlin. The undulator UE56/2 source delivered linearly polarised photons with a spectral resolution of $E/\Delta E = 2300$.

The two spectroscopy methods can be compared as such: With NEXAFS for a glancing angle of $\theta = 20^{o}$, excitations into π* orbitals are favoured over those into σ* orbitals. Thus, NEXAFS spectra for this glancing angle represent the experimental situation that occurs for reflection measurements at the same glancing angle with photon scattering in *p*-geometry.

Similarly at θ = 90º, σ* excitations are favoured, which approximates well the experimental situation that occurs for reflection measurements at θ = 20º and photon scattering in *s*-geometry. Here, in line with convention, for *p*-geometry the electric field vector of the x-ray light is in the plane that is spanned by beam and sample surface, whereas for *s*-geometry the electric field vector is perpendicular on this plane.

Between 288 eV and 291 eV, the reflectance for graphene could not be measured due to the dominance of higher order contributions of light coming from the monochromator.

Different HOPG samples were used for NEXAFS and reflectance measurements. A new HOPG surface was obtained by cleaving the sample with adhesive tape. The graphene sample was deposited on a copper foil substrate via chemical vapour deposition as described elsewhere [7]. The sample was furthermore annealed at 540 °C prior to the NEXAFS measurements. Due to instrumental constraints, such annealing could not be carried out before the reflectance measurements.

The Kramers-Kronig (KK) transformation used in this work utilized the program created by Watts [4]. This software segments the KK transformation [8] into piecewise Laurent polynomials. Importantly, it addresses effectively the need for a large set of equidistant data points to solve the integral from 0 to infinity and treats in (1) the undefined point with E'^2-E^2=0 as a Cauchy principal value. The real part of the atomic scattering factor may be expressed as

$$f_1(E) = Z^* - \frac{2}{\pi} P \int_0^\infty \frac{E' \cdot f_2(E')}{E'^2 - E^2} \delta E' \qquad (1)$$

The imaginary part of the atomic scattering factor, f_2, in this equation may be estimated for a given glancing angle from a NEXAFS measurement of the x-ray absorption in a sample. The real part of the atomic scattering factor, f_1, is then calculated using (1) employing an appropriate numerical approximation [4].

The atomic scattering factor (f_1, f_2) is related to the RI *n* and the associated extinction coefficient *k* as given below in (2).

$$1 - \frac{e^2 N_a}{2\pi m_e c^2} \lambda^2 \rho \frac{\sum_j x_j (f_{1j} + i f_{2j})}{\sum_j x_j A_j} = n + ik \qquad (2)$$

When the atomic composition x_j and also the respective atomic densities A_j in this equation are specified, a known atomic scattering factor (f_1, f_2) can be expressed in the form of the RI *n* and the associated extinction coefficient *k* [9]. After the RI has been expressed in this way, the x-ray reflectance of the sample, in *p*- (R_p) and *s*-geometry (R_s), can be calculated using the Fresnel equations [10]. The calculations of the reflectance were performed using the IMD software package [9].

3. Results

Figure 1 shows the energy-dependent *n*- and *k*-values calculated after the KK-transformation of the NEXAFS data for (a) HOPG and (b) graphene. The data show well pronounced resonant excitations at the π*- and σ*-resonances near 285 eV and 291 eV. For HOPG, additional resonances between 287 eV and 288 eV are likely due to carbonaceous surface adsorbates, since the sample was not annealed before measurement. Apart from this difference, the RI of HOPG and graphene are very similar and dominated by the π*- and σ*-resonances.

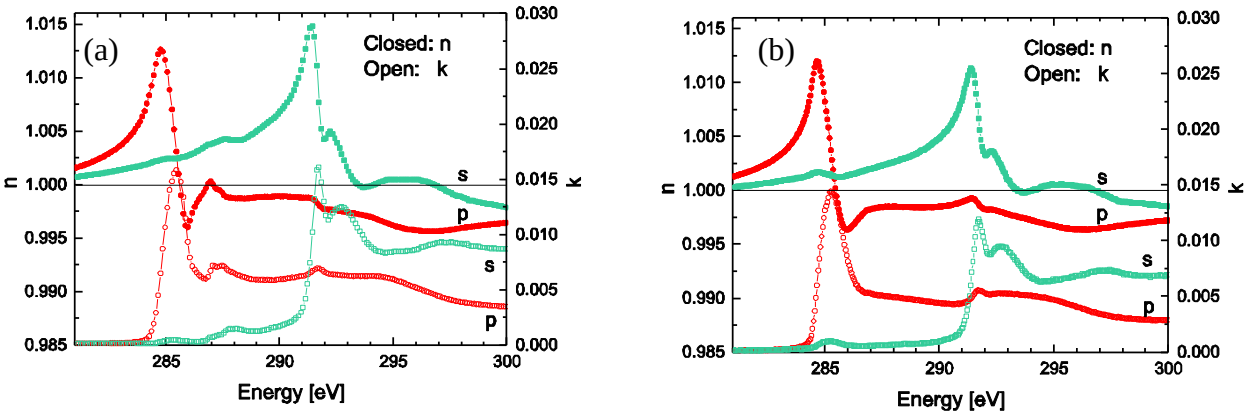

Fig. 1. RI experimental optical constant *n* and deduced extinction coefficient *k* of (a) HOPG and (b) graphene.

The calculated refractive indices were input in the Fresnel equations to simulate reflection spectra over the energy range from 280 eV to 300 eV. The simulated spectra are shown in Fig. 2 in comparison with experimental data. A prediction for amorphous carbon, based on the standard Henke data [11] is also shown as reference.

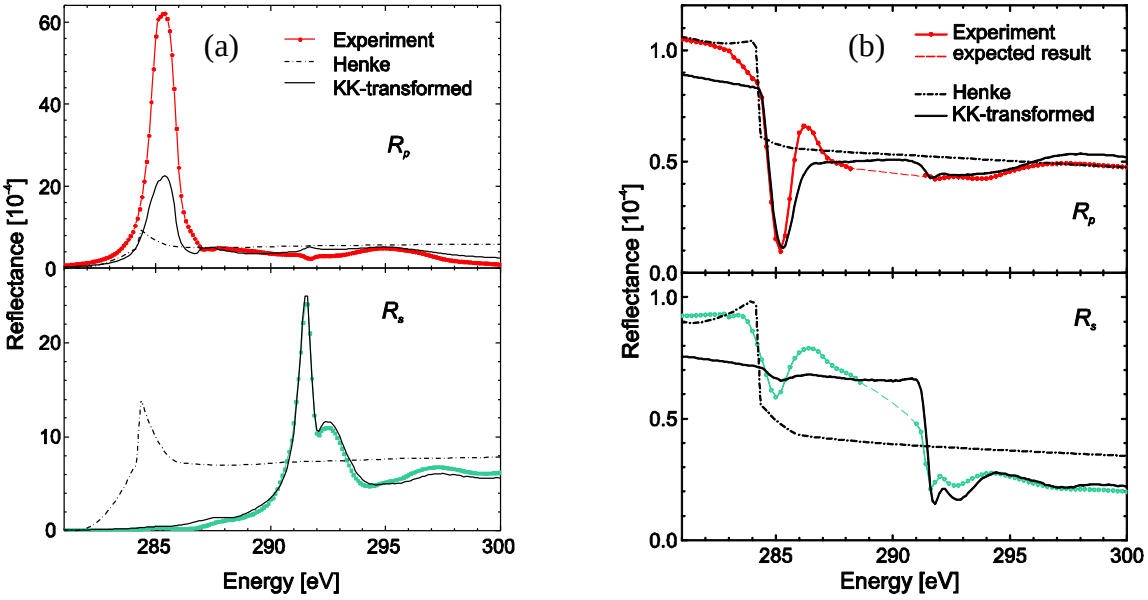

Fig. 2. Simulation of the measured reflectance for (a) HOPG and (b) graphene on copper using KK-transformed data (solid) and Henke data (dash-dot). In (b), between 288 eV and 291 eV, the reflectance is unknown due to the insensitivity of the measurement – the expected result is shown instead as dashed line.

For HOPG in (a), there is a qualitative agreement with the π*-resonance lineshape and an excellent reproduction of the σ*-resonance and its fine structure. The reduced intensity for the simulated π*-resonance may be due to the finite interface roughness [9] which was included to achieve a better fit above 287 eV (0.6 nm for R_p and 0 nm for R_s). The simulations using the Henke tables on the other hand show only step-like structures that poorly represent the measured reflectances and disregard the observed dichroism of graphite.

For graphene, the data from the Henke tables give a reasonable prediction of the non-resonant regions in Fig. 2(b), if the thickness of the carbon layer is set to 1 nm and 0.4 nm for R_p and R_s, respectively. For simulations using the KK-transformed RI of graphene different layer thicknesses were used (0.7 nm R_p, 0.3 nm R_s) and the measured reflectances, including fine structures near 285 eV in R_p and 292 eV in R_s, are then qualitatively represented.

Considering the inconsistent values for the graphene layer thickness, the agreement is, however, not as convincing as in the case of HOPG.

4. Conclusion

In this work realistic complex refractive indices have been deduced for HOPG and graphene on copper that include the natural dichroism of the materials. Whereas the resonant structures in HOPG are convincingly represented using simulations based on the new data, the measured graphene reflection spectra are not as well simulated. This is not unexpected, because the annealing before the NEXAFS measurement may have improved the structural integrity of the graphene layer and removed carbonaceous adsorbates. In contrast the reflectance measurements were performed without prior annealing. Additionally, unlike bulk-material as HOPG, interference effects can occur for the graphene-copper system that depend sensitively on layer thickness and affect the agreement of simulation and measurement. Nonetheless, reflectance measurements on both materials have confirmed the efficacy of the new approach with simulations predicting correctly expected differences between *p*- and *s*-geometry scattering. Furthermore the work has shown that the refractive indices of HOPG and graphene across the carbon K-edge are very similar.

Acknowledgments

We thank Bruce Cowie, Anton Tadich and Lars Thomsen of the soft x-ray beamline team at the Australian Synchrotron for their support. We acknowledge the financial and technical support from the Helmholtz-Zentrum Berlin. We are grateful to Ju-Hwan Kim for synthesizing the graphene on copper sample at Kyung Hee University in Korea.

References

[1] Joyeux D and Polack F 1998 *X-Ray Microscopy and Spectromicroscopy* ed J Thieme, G Schmahl, D Rudolph and E Umbach (Berlin Heidelberg : Springer-Verlag) p 207
[2] Mertins H-C, Schäfers F, Grimmer H, Clemens D, Böni P and Horisberger M 1998 *Appl. Opt.* **37**(10) 1873
[3] Yan H, Wang C, McCarn A R and Ade H 2013 *Phys. Rev. Lett.* **110**(17) 177401
[4] Watts B 2014 *Opt. Express* **22**(19) 23628
[5] Cowie B C C, Tadich A and Thomsen L 2010 *AIP Conf. Proc.***1234**(1) 307
[6] Schäfers F, Mertins H C, Gaupp A, Gudat W, Mertin M, Packe I et al 1999 *Appl. Opt.* **38**(19) 4074
[7] Chan Wook J, Ju Hwan K, Jong Min K, Dong Hee S, Sung K and Suk-Ho C 2013 *Nanotechnology* **24**(40) 405301
[8] Kronig R D L 1926 *J. Opt. Soc. Am.* **12**(6) 547
[9] Windt D L 1998 *Comput. Phys.* **12**(4) 360
[10] Attwood D 1999 *Soft X-Rays and Extreme Ultraviolet Radiation* (Cambridge University Press)
[11] Henke B L, Gullikson E M and Davis J C 1993 *At. Data Nucl Data Tables.* **54**(2) 181